CARBON 47 (2009) 3201–3207

available at www.sciencedirect.com

ScienceDirect

journal homepage: www.elsevier.com/locate/carbon

Ion irradiation and defect formation in single layer graphene

Giuseppe Compagnini[a,*], Filippo Giannazzo[b], Sushant Sonde[b,c], Vito Raineri[b], Emanuele Rimini[b,d]

[a]Department of Chemistry, University of Catania, Viale A. Doria 6, Catania 95123, Italy
[b]CNR-IMM, Strada VIII, 5, Catania 95121, Italy
[c]Scuola Superiore di Catania, Via San Nullo, 5/I, Catania 95123, Italy
[d]Department of Physics and Astronomy, University of Catania, Via S. Sofia 64, Catania 95123, Italy

ARTICLE INFO

Article history:
Received 18 June 2009
Accepted 10 July 2009
Available online 15 July 2009

ABSTRACT

Ion irradiation by 500 keV C^+ ions has been used to introduce defects into graphene sheets deposited on SiO_2 in a controlled way. The combined use of Raman spectroscopy and atomic force microscopy (AFM) allowed one to clarify the mechanisms of disorder formation in single layers, bilayers and multi-layers of graphene. The ratio between the D and G peak intensities in the Raman spectra of single layers is higher than for bilayers and multi-layers, indicating a higher amount of disorder. This cannot be only ascribed to point defects, originating from direct C^+–C collisions, but also the different interactions of single layers and few layers with the substrate plays a crucial role. As demonstrated by AFM, for irradiation at fluences higher than 5×10^{13} cm^{-2}, the morphology of single layers becomes fully conformed to that of the SiO_2 substrate, i.e. graphene ripples are completely suppressed, while ripples are still present on bilayer and multi-layers. The stronger interaction of a single layer with the substrate roughness leads to the observed larger amount of disorder.

1. Introduction

Carbon nanomaterials are becoming day by day much more important for basic science and applied technology. It is possible to obtain in a controlled way structures such as wires, tubes and sheets of arbitrary form and nearly arbitrary extension. In particular graphene [1], a two-dimensional (2D) sheet of carbon atoms arranged in a honeycomb lattice, attracted recently a huge scientific interest, due to its outstanding transport properties [2], chemical and mechanical stability and to the scalability of graphene devices to nano-dimensions [3].

The study of defects and impurities in single layer and few layers graphene is of crucial importance to understand and predict the behaviour of such material. In fact, the intentional/unintentional presence of those defects strongly affects the electronic transport properties of graphene devices [2]. Above and beyond, the controlled introduction of defects in graphene can be used to tailor physical, chemical and mechanical properties [4].

Recently, the effects of electron beam irradiation [5] and plasma treatments [6] on the crystalline order and on the electronic properties of graphene sheets have been investigated. Only few works have been reported on energetic ion irradiation in graphene [7]. However, no explanation on the defect formation on a so thin layer (monolayer) by keV ion irradiation has been given. The deposited energy is very low (mainly electronic loss) and the number of vacancies created by direct collisions negligible. Nevertheless, a relevant number of introduced defects is reported. Furthermore, ion irradiation by ion implanters represents the best and widely used way to introduce controlled amount of defects in solids and

* *Corresponding author:* Fax: +39 095580138.
E-mail address: gcompagnini@unict.it (G. Compagnini).
0008-6223/$ - see front matter © 2009 Elsevier Ltd. All rights reserved.
doi:10.1016/j.carbon.2009.07.033

can be used to locally (by focused ion beams or masking) induce modifications in graphene, such as the transition from sp^2 to sp^3 hybridization controlling locally the graphene/graphane [8] transition and approaching 2D band gap engineering. Ion irradiation of graphene is particularly interesting also because it allows to understand how the energy released by the single ion at the beginning of the collision cascade is planar distributed on such a single atomic carpet.

For all these reasons we started a series of microscopic and spectroscopic observations of ion irradiated graphene layers by changing both the number of piled-up layers involved in the irradiation and the density of the defects released by the ion beam through a strict control of the radiation fluence. In this work, single layer and few layers of graphene deposited on 100 nm SiO_2 grown on Si were irradiated with 500 keV C^+ ions at fluences ranging from 10^{13} to 10^{14} cm^{-2}. In the works reported to date in literature, low energy (few keV) ions have been used to irradiate graphene deposited on SiO_2. In that energy regime, the projected range of implanted ions is within few nanometers in the SiO_2. Hence, structural changes can happen in the SiO_2 surface region and influence the defect release in graphene. In our study, high energy C ions were used, since the projected range is very deep in the substrate below the SiO_2 layer, while the SiO_2 remains almost unaffected by the implantation. Raman spectroscopy and atomic force microscopy (AFM) were jointly applied to study the mechanisms of defect release on single and few layers of graphene.

2. Experimental details

Few layers of graphene were obtained by micromechanical exfoliation of HOPG [1] and deposited on a Si substrate coated with 100 nm thick oxide. As-prepared samples were implanted with 500 keV C^+ ions at four different fluences: 1×10^{13}, 2×10^{13}, 5×10^{13} and 1×10^{14} cm^{-2}. Implants were carried out under high vacuum conditions (10^{-6} Torr) in order to minimize surface contaminations.

The incident ion beam releases energy to the graphene layer by direct collisions with lattice C atoms and by interaction with electrons in the sheets. For 500 keV C^+ ions incident on a single layer of graphene, the cross section of direct C^+–C collisions can be estimated as $\sigma \approx 1\times10^{-17}$ cm^2. This simple estimation is based on the Kinchin-Pease theory of the displacement of atoms in solids by radiation [9] and on recent works on graphite irradiation [10]. Since the density of C atoms in graphene is $N \approx 4\times10^{15}$ cm^{-2}, the probability that a direct collision occurs, with the formation of a vacancy, is $N\sigma \sim 4\times10^{-2}$. Hence, the expected density of vacancies for ions fluences from 1×10^{13} to 1×10^{14} cm^{-2} is ranging from 4×10^{11} to 4×10^{12} cm^{-2}.

Both as prepared and implanted samples were preliminarily inspected by optical microscopy, in order to identify the few layer graphene flakes, and, hence, by tapping mode atomic force microscopy using a DI3100 equipment by Veeco with Nanoscope V electronics. AFM analyses allowed the morphological characterization and the identification of the number of layers in the flakes without causing structural damage [11,12]. In Fig. 1, typical AFM and optical images on a sample containing both monolayer (i) bilayer (ii) and multi-layer (iii) regions are reported.

Raman spectra were measured both on as-prepared and irradiated samples preliminarily identified by AFM. The measurements were performed at room temperature with a Jobin Yvon spectrometer using a 633 nm exciting radiation and a 3 cm^{-1} resolution. A 100× objective ensures a lateral resolution close to 1 μm (see spots on Fig. 1). Extreme care is taken to avoid sample damage or laser induced heating. Measurements were performed at 1 mW incident power. No significant spectral change was observed in such a configuration. We also measured the reference bulk graphite used to produce the layers.

3. Results and discussion

For a long time Raman spectroscopy has been considered the most powerful spectroscopic technique to study carbon based materials due to the specific response to any change in carbon hybridization state [13,14] as well as the introduction of defects [15] or foreign species [16]. In the specific case, the effects of ion irradiation on highly oriented graphite samples has been extensively studied by Dresselhaus et al. more than 20 years ago by Raman spectroscopy [17]. They observed that three regimes of behaviour can be achieved by evaluating the energy deposited into the collision cascade during the ions' slowing down inside the sample. At low fluences the disorder D line located at 1360 cm^{-1} starts to appear and its intensity grows quite linearly with the ion fluence. In this regime the D peak is sharp and is related with the appearance of pockets of disorder within ordered HOPG. At intermediate fluences the first order Raman peaks start to broaden because of the percolation of single disordered domains (sometimes called microcrystalline regime). At these first two stages, generally, annealing at moderate temperatures is able to restore the primitive order. A final stage can be obtained by further increasing the damage, thus leading to an amorphous carbon sample.

A similar scenario can be assumed to occur also during ion irradiation of single and few layers of graphene deposited on SiO_2, even if the threshold fluences between the mentioned three regimes are not exactly known in this case. Of course those thresholds values depend on the mass and energy of the irradiating ions. Since for C^+ ion irradiation at 500 keV, the coalescence of disorder pockets in HOPG (i.e. the transition from the first to the second regime) should occur at fluences higher than 5×10^{14} ions/cm^2, we have properly chosen a maximum fluence of 1×10^{14} ions/cm^2 in our experiment, in order to stay in the first regime. This is obviously the most intriguing one, because the long range integrity of the graphene layer is still maintained, but the introduced defects modify the electronic and mechanical properties of the sheet.

In Fig. 2 we report the Raman spectra obtained for different ion fluences in a single layer graphene. Beside the already mentioned D line, other three main features are to be considered. Two of them are observed even in the case of defects free graphite (HOPG). They are the G line at 1580 cm^{-1}, due to the doubly degenerate zone centre E_{2g} mode and the G' (or 2D) line, appearing in the range 2600–2800 cm^{-1} and

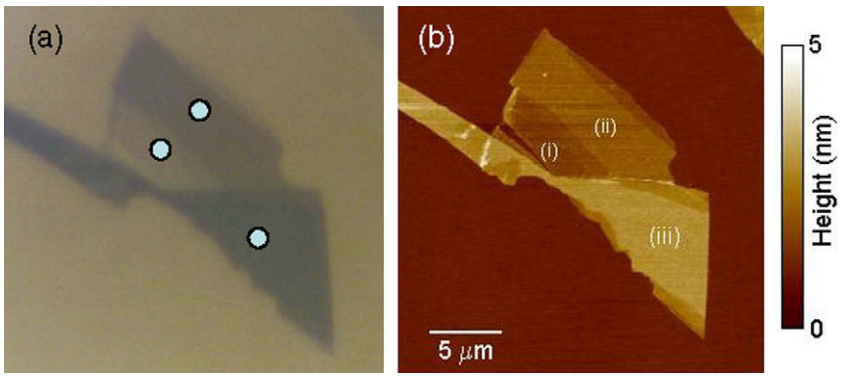

Fig. 1 – Typical optical (a) and AFM (b) images on a sample containing both monolayer (i) bilayer (ii) and multi-layer (iii) regions. The spots on the optical image indicate the spatial resolution of the Raman measurements.

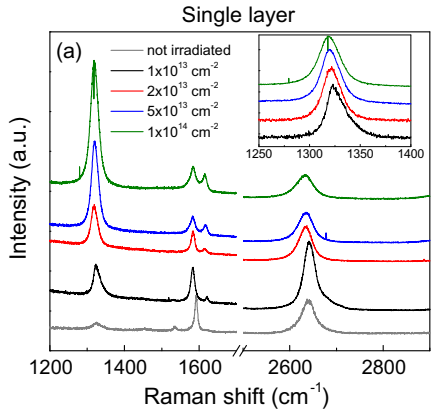

Fig. 2 – Raman spectra on a single layer graphene not irradiated and irradiated with 500 keV C ions at 1×10^{13}, 2×10^{13}, 5×10^{13} and 1×10^{14} cm^{-2} fluences. In the insert, the D peak for the four fluences is reported (here intensities are normalized).

corresponding to the overtone of the D band. The third signal is considered another defects induced Raman feature, it is frequently termed D' line and is located at 1620 cm^{-1}. The nature and the dispersive behaviour of D, D' and G' bands have been nicely correlated invoking the so called double resonance Raman process [18], recently applied also to the features observed in single and few layers graphene [19].

The introduction of controlled amount of defects through ion irradiation has notably consequences on most of the above mentioned Raman features for what concerns either the position and the relative intensities. As a first observation, the D line (see the inset of Fig. 2a) rises asymmetric at the lowest fluence and seems to red-shift and increase in width. These effects are specific for single layer graphene and have not been reported for 3D graphite structures. If one would invoke the double resonance theory the observation of a red-shift could be correlated with a change in the electronic structure of the layer due to the presence of defects or to an increasing strain in the graphene sheet.

Regarding the G' line we observe two apparently conflicting trends. On one side the intensity of G' decreases by increasing the ion irradiation fluence with respect to the G line, suggesting an approach to the "infinite layers" condition. On the other hand the second order structure continues to show a quite symmetrical line-shape like that always found in single layer graphene (Fig. 2b), while a redshift consistently scales with the D line behaviour.

A proper quantification of the amount of defects in graphite-like materials using Raman spectroscopy has been historically given through the evaluation of the size (L_a) of in-plane crystallites formed by a certain number of carbon rings [20] and this has been related to the I_D/I_G intensity ratio. It is now well established that there is a direct correlation between these two quantities as [15]:

$$L_a = (2.4\times10^{-10})\lambda_{laser}^4\left(\frac{I_D}{I_G}\right)^{-1} \quad (1)$$

here, λ_{laser} is the laser excitation wavelength expressed in nm as well as La. The original idea behind this was to link the *D* peak intensity to phonon confinement. Thus, since the *G* peak is the allowed phonon, the intensity of the not allowed phonon would be ruled by the "amount of breaking" of the selection rule. If this relation, generally observed for nanographites, is considered valid also for a single graphene layers, an irradiation at 10^{14} ions/cm^2 would lead to the formation of graphitic domains of the order of 5 nm, that is few hundreds of fused carbon rings.

It is important to observe that ion irradiation of 3D ordered graphite (HOPG) in similar conditions [17] never leads to I_D/I_G values as high as those given in the spectra reported in Fig. 2 (up to 7) with such sharp D and G bands (see Fig. 3 in Ref. [10]). This opens the question whether or not the above mentioned relation could be applied to a single graphene sheet or something peculiar is happening in such a 2D structure. In any case the sharpness of the disorder induced bands shown in Fig. 2, even for samples with very small crystallite sizes, reveals well-defined boundaries for the crystallites and their narrow size distribution.

The persistence of sharp D and G features can be correlated to the absence of percolation between single disorder domains in such a way to induce a picture in which the presence of different layers is essential for such a percolation behaviour or that there is a direct effect of the underlying SiO_2 substrate.

In order to clarify which is the role of graphene interaction with the SiO_2 substrate during ion irradiation, atomic force

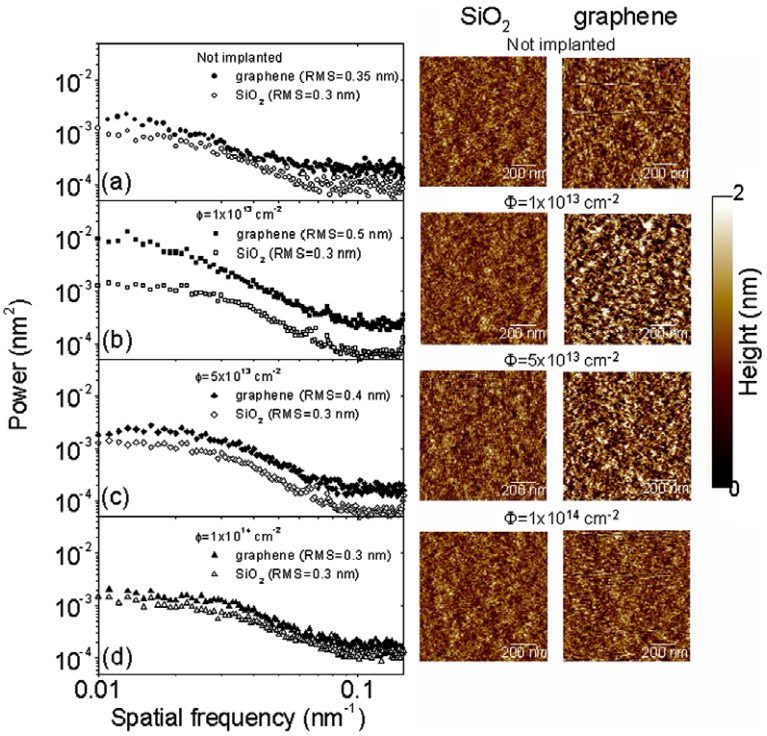

Fig. 3 – AFM images acquired on 1×1 μm scan areas on SiO_2 and supported graphene for not irradiated samples and for irradiated (fluences of 1×10^{13}, 5×10^{13} and 1×10^{14} cm^{-2}). Power spectra of the AFM maps were calculated for all the samples and reported in Fig. 3a–d.

microscopy (AFM) was used. The possibility to introduce a controlled density of defects in supported graphene sheets without destroying the long range crystalline order allowed also to study how the morphology of the 2D crystal changes to maintain stability in the presence of those defects. It has been demonstrated that the thermodynamic stability of exfoliated graphene from HOPG depends on its peculiar nanoscale corrugation [21]. The rippled shape of the 2D sheets has been proved experimentally both on free-standing graphene and on graphene supported by a substrate [22]. In the latter case it has been shown that, on nanoscale, graphene is only partially conformal to the substrate morphology and exhibits intrinsic ripples. Hence, it is worth to understand how graphene morphology changes with increasing the defect density in the sheet. To this aim, a systematic comparison was carried out between the surface morphologies of single layer graphene and bare SiO_2 both in the not irradiated samples and in the irradiated ones at different fluences. The results are summarized in Fig. 3, where the AFM images acquired on 1×1 μm scan areas on SiO_2 and supported graphene are reported for not irradiated samples and for irradiated ones with ion fluences of 1×10^{13}, 5×10^{13} and 1×10^{14} cm^{-2}. While the SiO_2 surface is unaffected by the high energy (500 keV) C^+ irradiation, changes in the surface corrugation of graphene are clearly evident, depending on the ion fluence.

To perform a quantitative comparison of these data, the power spectra of the AFM maps were calculated for all the samples and reported in Fig. 3a–d. They are obtained performing the Fast Fourier transform (FFT) of each map and plotting the square of the amplitude versus the spatial frequency. The root mean square roughness (RMS) of the surface is defined as the square root of the integral of the power over the considered frequency range. The power spectral analysis allows to distinguish how features of different lateral size on the surface (i.e. different spatial frequency in the power spectra) contribute to the RMS roughness. In Fig. 3 the power spectra on graphene surface are compared with those on the bare SiO_2 surface in order to disentangle the graphene corrugation from that of the underlying SiO_2 substrate. As deposited graphene weakly adheres on SiO_2 (with a van der Waals interaction) and its morphology follows only partially that of the substrate, as confirmed the power spectra in Fig. 3a. Power values on graphene are a factor of 2 higher than on SiO_2 for spatial frequencies between 0.01 and 0.03 nm^{-1} (i.e. features on graphene with lateral dimensions between 30 and 100 nm are about 1.4 times higher than on SiO_2) and a factor of 4 higher for spatial frequencies lower than 0.04 nm^{-1} (i.e. features on graphene with lateral dimensions lower than 25 nm are about 2 times higher than on SiO_2). It is worth noting that, after irradiation with a fluence of 1×10^{13} cm^{-2}, the power on graphene is almost a factor of 10 higher than on SiO_2 in the entire frequency range (see Fig. 3b). It is reasonable that, during irradiation, part of the weak bounds between graphene and the substrate are broken and a larger fraction of graphene surface becomes free-standing with respect to SiO_2 one. Such an effect has been observed in the literature for high energy proton irradiation of graphene on SiO_2, even using very low fluences (10^{11} cm^{-2}) not causing defects formations (no D peak in the Raman spectra) [23]. The most interesting and new effect observed in this experiment is the decrease in graphene power spectra at fluences higher than 5×10^{13} cm^{-2} (see Fig. 3c and d). In particular, after irradiation at the highest fluence

(1×10^{14} cm^{-2}), graphene and SiO_2 power spectra are almost superimposed. This indicates that, increasing the defect density in graphene above a certain threshold, graphene ripples are strongly suppressed and the defected crystal maintains its thermodynamic stability by adapting its shape to that of the substrate.

Fig. 4 reports differences in the Raman spectra taken after 10^{14} ions/cm^2 irradiation in a single-, double- and multi-layer graphene. It clearly shows that the I_D/I_G intensity ratio depends on the number of irradiated layers, i.e. it is higher by decreasing the number of layers. This means that the production of defects into a single graphene layer due to ion irradiation is strongly influenced by the presence of one or more underlying planes. This is plausible since in the case of a multi-layer system the same ion, in its collision cascade, induces defects in a very large number of planes around the same spatial region. These defects are free to evolve and interact each other during the cascade quenching [24]. The same Fig. 4 reports changes in the D line position and width by changing the number of layers involved, while in Fig. 5 a correlation between the I_D/I_G intensity ratio and the ion fluence if given for different layered systems.

In this respect, it is generally agreed that during an ion irradiation process the surface damage occurs on a random basis. Hence, the I_D/I_G ratio as a function of the ion fluence which can be fitted with functions like:

$$\frac{I_D}{I_G} = \left(\frac{I_D}{I_G}\right)_{sat}(1-e^{-\eta\varphi}) \qquad (2)$$

where $(I_D/I_G)_{sat}$ is the ratio at its saturation value and φ is the ion fluence. The parameter η is defined as the disorder release efficiency in the layer, which in single layer graphene ion irradiation is ~3 times more efficient in the production of disorder than in multi-layer. A way to interpret these results, in the frame of an interaction between the created defects, is to imagine that for bi- and multi-layer systems a knocked out carbon atom cannot be entirely ejected from the system.

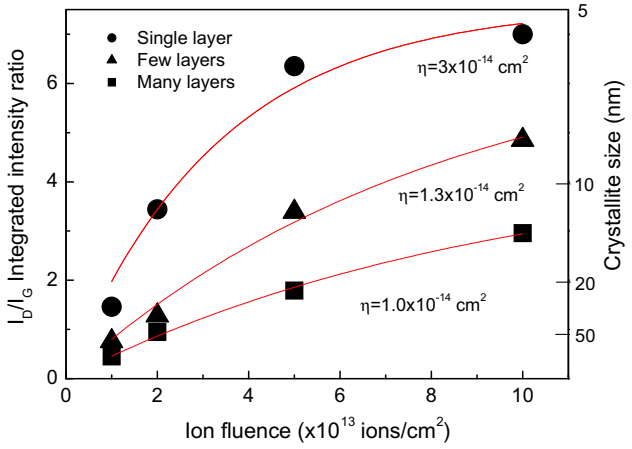

Fig. 5 – Ratio of the D peak and G peak intensities (I_D/I_G) as a function of the ion fluence for a single layer, a double layer and a multi-layer of graphene.

Particularly for partial/oblique collisions the atoms could be captured between the layers, allowing them to migrate and heal vacant sites [4].

As a final comment, the obtained results allow also to share light onto a relevant question regarding the nature of the G' structure in Raman spectra of graphite related materials. As previously mentioned, there is a general agreement in considering that the evolution of the G' lineshape by changing the number of layers involved in the probed scattering experiment can be explained with the so called 'double resonance' theory which links the phonon wavevectors to the electronic band structure. We have here the possibility to directly compare the D and G' lines in singles as well as double layer graphene possessing controlled amount of defects. For this reason we report in Fig. 6 the G' structure for the irradiated (10^{13} ions/cm^2) single and double layers together with the sig-

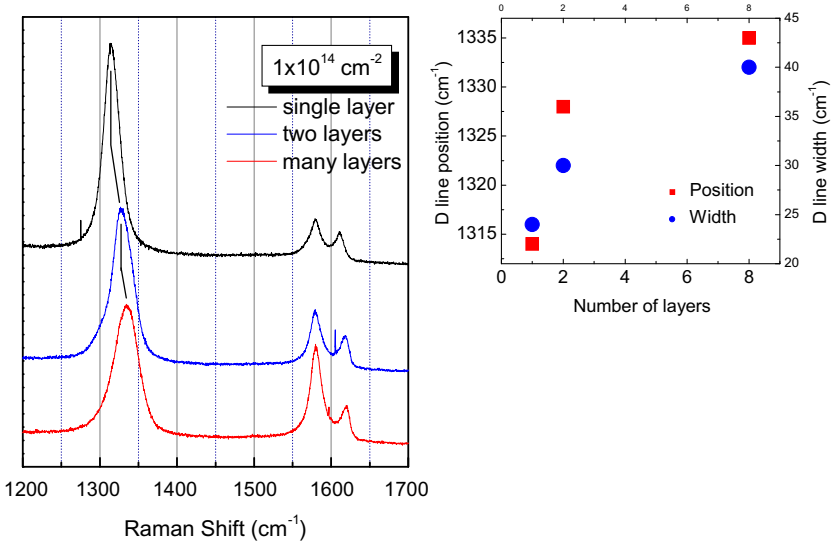

Fig. 4 – Raman spectra taken after 2×10^{13} ion/cm^2 irradiation in a single-, double- and multi-layer graphene pieces together with the spectrum of an as prepared single layer graphene.

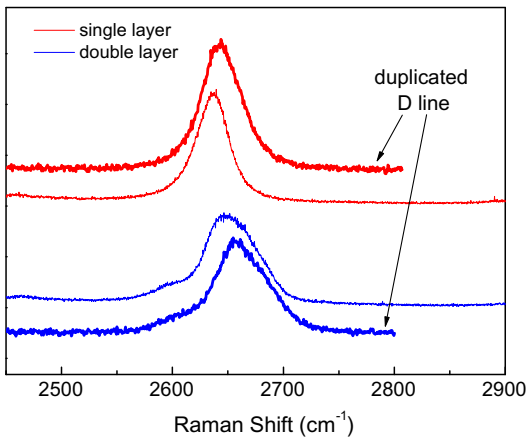

Fig. 6 – G' peak for the irradiated (10^{13} ions/cm^2) single and double layers together with the signals obtained in the D line region, duplicated in frequency to compare them with the second order signal.

nals obtained in the D line region, duplicated in frequency to compare them with the second order signal. As a first consideration we observe a shift between the second order signal and the duplicated one of about 5 cm^{-1} due to anharmonicity both in the case of single and double graphene layers. This is indeed the first experimental observation of anharmonicity in single and double layer graphenes ever reported. Regarding the single layer, the duplicated D line (36 cm^{-1}) has a width comparable with the respective G' structure (40 cm^{-1}) and can be deconvolved in the same four components as those needed for G'.

4. Conclusion

Ion irradiation by 500 keV C^+ ions has been used to introduce defects into graphene sheets deposited on SiO_2 in a controlled way. The combined use of Raman spectroscopy and atomic force microscopy (AFM) allowed to clarify the mechanisms of disorder formation in single layers, bilayers and multi-layers of graphene. The ratio between the D and G peak intensities in single layers are higher than on bilayers and multi-layers, indicating a higher amount of disorder. This cannot be ascribed to point defects, originating from direct C^+–C collisions, but is due to the different interaction between single layers and few layers with the substrate, as demonstrated by AFM analyses. In particular, for irradiation at fluences higher than 5×10^{13} cm^{-2}, graphene ripples are strongly suppressed and the defected crystal maintains its thermodynamic stability by adapting its shape to that of the substrate.

Acknowledgements

The authors want to acknowledge A. Marino and S. Di Franco from CNR-IMM, Catania, for their expert assistance in ion irradiation and in sample preparation and S. Trusso for the help in Raman measurements. This work has been partially supported by MUR (PRIN project 2007).

REFERENCES

[1] Novoselov KS, Geim AK, Morozov SV, Jiang D, Zhang Y, Dubonos SV, et al. Electric field effect in atomically thin carbon films. Science 2004;306:666–9.
[2] Chen JH, Jang C, Xiao S, Ishigami M, Fuhrer MS. Intrinsic and extrinsic performance limits of graphene devices on SiO_2. Nat Nanotechnol 2008;3:206–9.
[3] Han MY, Ozyilmaz B, Zhang Y, Kim P. Energy band-gap engineering of graphene nanoribbons. Phys Rev Lett 2007;98. p. 206805-1–4.
[4] Krasheninnikov AV, Banhart F. Engineering of nanostructured carbon materials with electron or ion beams. Nat Mater 2007;6:723–33.
[5] Teweldebrhan D, Balandin AA. Modification of graphene properties due to electron-beam irradiation. Appl Phys Lett 2009;94. p. 013101-1–3.
[6] Kim K, Park HJ, Woo BC, Kim KJ, Kim GT, Yun WS. Electric property evolution of structurally defected multilayer graphene. Nano Lett 2008;8:3092–6.
[7] Tapasztó L, Dobrik G, Nemes-Incze P, Vertesy G, Lambii P, Biró LP. Tuning the electronic structure of graphene by ion irradiation. Phys Rev B 2008;78. p. 233407-1–4.
[8] Elias DC, Nair RR, Mohiuddin TMG, Morozov SV, Blake P, Halsall MP, et al. Control of graphene's properties by reversible hydrogenation: evidence for graphane. Science 2009;323:610–3.
[9] Kinchin GH, Pease RS. The displacement of atoms in solids by radiation. Rep Prog Phys 1955;18:1–51.
[10] Nakamura K, Kitajima M. Ion-irradiation effects on the phonon correlation length of graphite studied by Raman spectroscopy. Phys Rev B 1992;45:78–82.
[11] Giannazzo F, Sonde S, Raineri V, Rimini E. Screening length and quantum capacitance in graphene by scanning probe microscopy. Nano Lett 2009;9:23–9.
[12] Sonde S, Giannazzo F, Raineri V, Rimini E. Dielectric thickness dependence of capacitive behavior in graphene deposited on silicon dioxide. J Vac Sci Technol B 2009;27:868–73.
[13] Scuderi V, Scalese S, Bagiante S, Compagnini G, D'Urso L, Privitera V. Direct observation of the formation of linear C chain/carbon nano tube hybrid systems. Carbon 2009;47:2134–7.
[14] D'Urso L, Compagnini G, Puglisi O. sp/sp^2 bonding ratio in sp rich amorphous carbon thin films. Carbon 2006;44:2093–6.
[15] Pimenta MA, Dresselhaus G, Dresselhaus MS, Cancado LG, Jorio A, Saito R. Studying disorder in graphite-based systems by Raman spectroscopy. Phys Chem Chem Phys 2007;9:1276–91.
[16] Calcagno L, Compagnini G, Foti G, Grimaldi MG, Musumeci P. Carbon clustering in $Si_{1-x}C_x$ formed by ion implantation. Nucl Instrum Methods 1996;B120:121–4.
[17] Elman BS, Dresselhaus MS, Dresselhaus G, Mby EW, Mazurek H. Raman scattering from ion implanted graphite. Phys Rev B 1981;24:1027–34.
[18] Saito R, Jorio A, Souza Filho AG, Dresselhaus G, Dresselhaus MS, Pimenta MA. Probing phonon dispersion relations of graphite by double resonance Raman scattering. Phys Rev Lett 2002;88. p. 027401-1–4.
[19] Ferrari AC, Meyer JC, Scardaci V, Casiraghi C, Lazzeri M, Mauri F, et al. Raman spectrum of graphene and graphene layers. Phys Rev Lett 2006;97. p. 187401-1–4.
[20] Tuinstra F, Koenig JL. Raman spectrum of graphite. J Phys Chem 1970;53:1126–31.
[21] Meyer JC, Geim AK, Katsnelson MI, Novoselov KS, Booth TJ, Roth S. The structure of suspended graphene sheets. Nature 2007;446:60–3.

[22] Geringer V, Liebmann M, Echtermeyer T, Runte S, Schmidt M, Ruckamp R, et al. Intrinsic and extrinsic corrugation of monolayer graphene deposited on SiO_2. Phys Rev Lett 2009;102. p. 076102-1–4.
[23] Stolyarova E, Stolyarov D, Bolotin K, Ryu S, Liu L, Rim KT, et al. Observation of graphene bubbles and effective mass transport under graphene films. Nano Lett 2009;9:332–7.
[24] Ewels CP, Telling RH, El-Barbary AA, Heggie MI, Briddon PR. Metastable Frenkel pair defect in graphite: source of Wigner energy. Phys Rev Lett 2003;91. p. 025505-1–4.